

# Interactions between Metal Ions and Carbohydrates. Spectroscopic Characterization and the Topology Coordination Behavior of Erythritol with Trivalent Lanthanide Ions

Limin Yang,<sup>\*,†</sup> Xiaohui Hua,<sup>‡</sup> Junhui Xue,<sup>†,§</sup> Qinghua Pan,<sup>‡</sup> Lei Yu,<sup>‡</sup> Weihong Li,<sup>‡</sup> Yizhuang Xu,<sup>\*,‡</sup> Guozhong Zhao,<sup>||</sup> Liming Liu,<sup>||</sup> Kexin Liu,<sup>†</sup> Jia'er Chen,<sup>†</sup> and Jinguang Wu<sup>‡</sup>

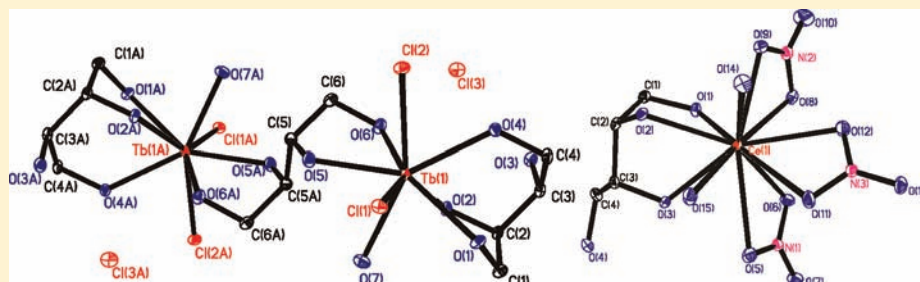
<sup>†</sup>State Key Laboratory of Nuclear Physics and Technology, Institute of Heavy Ion Physics, School of Physics, Peking University, Beijing 100871, China

<sup>‡</sup>Beijing National Laboratory for Molecular Sciences, State Key Laboratory for Rare Earth Materials Chemistry and Applications, College of Chemistry and Molecular Engineering, Peking University, Beijing 100871, China

<sup>§</sup>College of Chemical Engineering, Inner Mongolia University of Technology, Hohhot 010051, China

<sup>||</sup>Department of Physics, Capital Normal University, Beijing 100037, China

## Supporting Information



**ABSTRACT:** The coordination of carbohydrate to metal ions is important because it may be involved in many biochemical processes. The synthesis and characterization of several novel lanthanide-erythritol complexes ( $\text{TbCl}_3 \cdot 1.5\text{C}_4\text{H}_{10}\text{O}_4 \cdot \text{H}_2\text{O}$  (TbE(I)),  $\text{Pr}(\text{NO}_3)_3 \cdot \text{C}_4\text{H}_{10}\text{O}_4 \cdot 2\text{H}_2\text{O}$  (PrEN),  $\text{Ce}(\text{NO}_3)_3 \cdot \text{C}_4\text{H}_{10}\text{O}_4 \cdot 2\text{H}_2\text{O}$  (CeEN),  $\text{Y}(\text{NO}_3)_3 \cdot \text{C}_4\text{H}_{10}\text{O}_4 \cdot \text{C}_2\text{H}_5\text{OH}$  (YEN),  $\text{Gd}(\text{NO}_3)_3 \cdot \text{C}_4\text{H}_{10}\text{O}_4 \cdot \text{C}_2\text{H}_5\text{OH}$  (GdEN)) and  $\text{Tb}(\text{NO}_3)_3 \cdot \text{C}_4\text{H}_{10}\text{O}_4 \cdot \text{C}_2\text{H}_5\text{OH}$  (TbEN) are reported. The structures of these complexes in the solid state have been determined by X-ray diffraction. Erythritol is used as two bidentate ligands or as three hydroxyl group donor in these complexes. FTIR spectra indicate that two kinds of structures, with water and without water involved in the coordination sphere, were observed for lanthanide nitrate-erythritol complexes. FIR and THz spectra show the formation of metal ion-erythritol complexes. Luminescence spectra of Tb-erythritol complexes have the characteristics of the Tb ion.

## INTRODUCTION

The interaction between carbohydrates and metal ions is of increasing interest as it occurs during many important biological processes involving structural support in membrane systems, cell–cell adhesion, and transmission of nerve impulses.<sup>1–3</sup> The coordination of carbohydrates to metal ions plays an important role in biosyntheses, including metal transportation and storage and the regulation of metalloenzymes.<sup>4–7</sup> Metal–carbohydrate interactions have also been exploited in metal-catalyzed enantioselective synthesis. Metal–carbohydrate complexes are used as potential radiopharmaca, cancerostatica, imaging reagents, and catalysts for the production of hydrogen from sugars.<sup>8–17</sup> Metal-based glyconanoparticles (GNPs) are useful biofunctional nanomaterials.<sup>18</sup> When the concentration of  $\text{Ca}^{2+}$  is relatively low,  $\text{Ca}^{2+}$  prefers to coordinate with the carbohydrate moiety of mucin in the interactions between metal ions and glycoprotein.<sup>19</sup> However, relatively few papers about the crystal structures of metal–carbohydrate complexes have been

published in the literature because it is hard to prepare these metal complexes in the neutral state for the weak binding between metal ions and hydroxyl groups.

Lanthanide ions and calcium ions have relatively stronger interactions with carbohydrates. Lanthanide compounds are used as catalysts for the cleavage of RNA and DNA or as luminescence probes of calcium ion in biology,<sup>20–22</sup> or used in medicine; for example, lanthanum carbonate is used as a phosphate binder.<sup>23,24</sup> Since the applications are related to the interaction between lanthanide ions and biological ligands, the study of the binding modes of lanthanide ions with carbohydrates is of great interest.

Here, erythritol ( $\text{C}_4\text{H}_{10}\text{O}_4$ , denoted as E), one of the simplest representatives of carbohydrates, was chosen as a model to study the coordination behavior of hydroxyl groups to

Received: September 8, 2011

Published: December 8, 2011

metal ions. The investigation of the interactions between metal ions and simple sugars can improve the understanding of metal ion interactions with sugar residues of biologically important compounds and, consequently, the physiological role of metal ions, which needs to assign the binding hydroxyl or other groups, the changes of hydrogen bonds, and also to characterize the metal ion coordination of carbohydrates monitoring the ligand conformation and configuration changes forced by the complexation processes. Erythritol, galactitol, inositol, cyclohexanetriols and ribose, and so forth are often used as simple models to study the interactions between metal ions and carbohydrates.<sup>25–39</sup> Different ligands have various coordination modes, and one ligand may have several coordination modes: for example, galactitol may be used as two three-hydroxyl-group donor or two bidentate ligands to form a chain structure; or it may coordinate to four metal ions with its O-1 to one metal ion, O-2, -3 to the second metal ion, O-4, -5 with the third metal ion, and O-6 to the fourth metal ion to form a network structure.<sup>25–30</sup> Erythritol has four hydroxyl groups, and it may be used as three hydroxyl group donor or two bidentate ligands.<sup>40–45</sup> In this paper, new topological structures have been observed for lanthanide chloride and nitrate-erythritol complexes. Because single crystals of metal-sugar complexes are difficult to prepare, IR spectroscopy is a useful method to deduce unknown structures, so here the relationship between IR spectroscopy and structures was also discussed.

## EXPERIMENTAL SECTION

**Materials.**  $\text{TbCl}_3$  was prepared and crystallized from corresponding rare earth oxide of high purity (99.99%) with HCl.  $\text{Y}(\text{NO}_3)_3$ ,  $\text{Ce}(\text{NO}_3)_3$ ,  $\text{Pr}(\text{NO}_3)_3$ ,  $\text{Gd}(\text{NO}_3)_3$ , and  $\text{Tb}(\text{NO}_3)_3$  were purchased from a chemical reagent company in Shanghai. Erythritol was purchased from Acros, and was used without further purification.

**Preparation of  $\text{TbCl}_3 \cdot 1.5\text{C}_4\text{H}_{10}\text{O}_4 \cdot \text{H}_2\text{O}$  (TbE(I)),  $\text{Pr}(\text{NO}_3)_3 \cdot \text{C}_4\text{H}_{10}\text{O}_4 \cdot 3\text{H}_2\text{O}$  (PrEN),  $\text{Ce}(\text{NO}_3)_3 \cdot \text{C}_4\text{H}_{10}\text{O}_4 \cdot 3\text{H}_2\text{O}$  (CeEN),  $\text{Y}(\text{NO}_3)_3 \cdot \text{C}_4\text{H}_{10}\text{O}_4 \cdot \text{C}_2\text{H}_5\text{OH}$  (YEN),  $\text{Gd}(\text{NO}_3)_3 \cdot \text{C}_4\text{H}_{10}\text{O}_4 \cdot \text{C}_2\text{H}_5\text{OH}$  (GdEN), and  $\text{Tb}(\text{NO}_3)_3 \cdot \text{C}_4\text{H}_{10}\text{O}_4 \cdot \text{C}_2\text{H}_5\text{OH}$  (TbEN).** 3 mmol erythritol and 3 or 6 mmol metal chlorides or nitrates were dissolved in  $\text{H}_2\text{O}$ /ethanol and heated on a water bath at about 80 °C. Small aliquots of EtOH (Analytical Reagent) were periodically added to the solution during the heating process to prolong the reaction time, leading to the formation of these complexes. Then, the concentrated solutions were cooled down for crystallization. Anal. Calcd for TbE ( $\text{TbCl}_3 \cdot 1.5\text{C}_4\text{H}_{10}\text{O}_4 \cdot \text{H}_2\text{O}$ ): C, 15.45; H, 3.67. Found: C, 14.90; H, 3.73. Anal. Calcd for PrEN ( $\text{Pr}(\text{NO}_3)_3 \cdot \text{C}_4\text{H}_{10}\text{O}_4 \cdot 2\text{H}_2\text{O}$ ): C, 9.90; H, 2.91; N, 8.66. Found: C, 9.99; H, 2.87; N, 8.69. Anal. Calcd for CeEN ( $\text{Ce}(\text{NO}_3)_3 \cdot \text{C}_4\text{H}_{10}\text{O}_4 \cdot 2\text{H}_2\text{O}$ ): C, 9.92; H, 2.91; N, 8.68. Found: C, 9.88; H, 2.88; N, 8.76. Anal. Calcd for YEN ( $\text{Y}(\text{NO}_3)_3 \cdot \text{C}_4\text{H}_{10}\text{O}_4 \cdot \text{C}_2\text{H}_5\text{OH}$ ), C, 16.26; H, 3.64; N, 9.48. Found: C, 15.65; H, 3.595; N, 9.395. Anal. Calcd for TbEN:  $\text{Tb}(\text{NO}_3)_3 \cdot \text{C}_4\text{H}_{10}\text{O}_4 \cdot \text{C}_2\text{H}_5\text{OH}$ : C, 14.05; H, 3.14; N, 8.19. Found: C, 13.84; H, 3.16; N, 8.16.  $\text{Gd}(\text{NO}_3)_3 \cdot \text{C}_4\text{H}_{10}\text{O}_4 \cdot \text{C}_2\text{H}_5\text{OH}$ : C, 14.09; H, 3.15; N, 8.22. Found: C, 13.93; H, 3.23; N, 8.19.

**Physical Measurements.** Data for  $\text{Tb}(\text{NO}_3)_3 \cdot \text{C}_4\text{H}_{10}\text{O}_4 \cdot \text{C}_2\text{H}_5\text{OH}$  was made on a Rigaku R-AXIS RAPID IP spectrometer using monochromatic Mo  $K\alpha$  radiation ( $\lambda = 0.71073 \text{ \AA}$ ) at 293(2) K. The structure was resolved by direct methods with SHELX-97 and refined using the full-matrix least-squares on the  $F^2$  method. Empirical absorption corrections were applied and anisotropic thermal parameters were used for the non-hydrogen atoms and isotropic parameters for the hydrogen atoms. Hydrogen atoms were added geometrically and refined using a riding model.<sup>46</sup> Data for TbE(I), PrEN, CeEN, YEN, and GdEN were collected on a Rigaku Saturn 724 spectrometer equipped with graphite-monochromatized Mo  $K\alpha$  radiation ( $\lambda = 0.71073 \text{ \AA}$ ) at 173(2) K. The methods used to resolve the crystal structures are similar to TbEN. The crystal data and

structure refinements of these metal-erythritol complexes are listed in Table 1.

The mid-IR spectra were measured on a Nicolet Magna IN10 spectrometer using micro-IR method at  $4 \text{ cm}^{-1}$  resolution. Element analyses were carried out on an Elementar Vario EL spectrometer. The THz absorption spectra were recorded on the THz time-domain device of Capital Normal University of China, based on photo-conductive switches for generation and electro-optical crystal detection of the far-infrared light. The experimental apparatus for terahertz transmission measurements has been discussed in detail elsewhere.<sup>47</sup> The preparation of the samples was by pressing mixed pellets with polyethylene powder; the thickness of the samples is about 0.8 mm. The detection of THz absorption spectra was carried out in  $\text{N}_2$  atmosphere to avoid the influence of water vapor. The far-IR spectra of the molecules in the  $650\text{--}50 \text{ cm}^{-1}$  region were measured using commonly used Nujol mull method and were taken on a Nicolet Magna-IR 750 II Spectrometer at room temperature and at  $8 \text{ cm}^{-1}$  resolution, 128 scans. The luminescence spectra of TbE(I) and TbEN were measured on a Hitachi F4500 luminescence spectrometer.

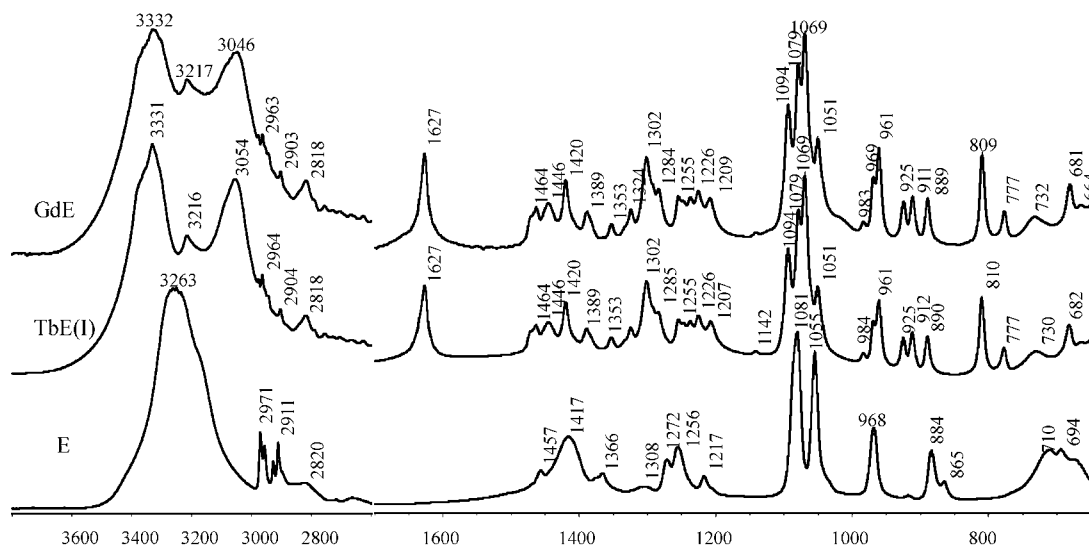
## RESULTS AND DISCUSSION

**Structure of Lanthanide Chloride-Erythritol Complexes, TbE(I).** The FTIR spectra of erythritol, TbE(I), and GdE were shown in Figure 1. Compared to the IR spectrum of erythritol, the changes in the IR spectra of TbE(I) and GdE indicate the formation of new lanthanide chloride-erythritol complexes. In fact, four lanthanide chloride-erythritol complexes have been obtained;<sup>40–45</sup> it is amazing that there is still one new IR spectrum that can be obtained. For the spectrum of TbE(I), in the  $3800\text{--}2600 \text{ cm}^{-1}$  region, 3331, 3216, and  $3054 \text{ cm}^{-1}$  bands were observed, which are related to the hydrogen bond networks after complexation. Weak bands at 2964, 2904, and  $2818 \text{ cm}^{-1}$  are related to  $\nu\text{CH}$ . The changes in peak positions and the decrease of relative intensities of  $\nu\text{CH}$  indicate the formation of metal complexes and rearrangement of CH chain. Usually,  $\delta\text{H}_2\text{O}$  is located at  $\sim 1644 \text{ cm}^{-1}$ .<sup>48</sup> It has shifted to  $1627 \text{ cm}^{-1}$  corresponding to coordinated water molecules in TbE(I), which indicate that coordinated water molecules exist in its structure. The peak positions and relative intensities of the bands in the  $1500\text{--}650 \text{ cm}^{-1}$  region change compared to those of erythritol itself, which indicate the formation of metal complex.  $\delta\text{CH}_2$  has shifted to  $1464 \text{ cm}^{-1}$  for TbE(I).

In addition, 1081 and  $1055 \text{ cm}^{-1}$  bands (mainly  $\nu\text{CO}$  vibrations) in erythritol are shifted to 1094, 1079, 1069, and  $1051 \text{ cm}^{-1}$  in TbE(I), which indicates coordination of hydroxyl groups to the  $\text{Tb}^{3+}$  ion. By comparison of the IR spectrum of TbE(I) in the  $1500\text{--}650 \text{ cm}^{-1}$  region with other lanthanide-erythritol complexes, when erythritol has two coordination modes in one system, their IR spectra usually have more bands (TbE(I) and NdE(II)), and when erythritol only has one coordination mode (PrE, PrEN, and TbEN), the number of the bands in their IR spectra is relatively limited. For example, for TbE(I), 28 bands at 1464, 1446, 1420, 1389, 1353, 1325, 1302, 1285, 1255, 1248, 1237, 1226, 1207, 1142, 1094, 1079, 1069, 1051, 984, 969, 961, 925, 912, 890, 810, 777, 730, and  $682 \text{ cm}^{-1}$  were observed. For NdE(II), 27 bands at 1470, 1456, 1434, 1415, 1385, 1363, 1351, 1331, 1282, 1271, 1252, 1232, 1216, 1120, 1102, 1075, 1068, 1042, 1031, 987, 964, 924, 895, 875, 817, 777, and  $681 \text{ cm}^{-1}$  were observed. For PrE, only 15 bands at 1469, 1441, 1427, 1399, 1321, 1288, 1243, 1218, 1073, 1058, 1049, 968, 902, 804, and  $752 \text{ cm}^{-1}$  were observed. So, we can estimate that one or two coordination modes appear according to the number of the

Table 1. Crystal Data and Structure Refinement for TbE(I), CeEN, PrEN, YEN, GdEN, and TbEN

	TbE (I)	CeEN	PrEN	YEN	GdEN	TbEN
CCDC No.	833813	839234	826190	839238	839233	791955
chemical formula	C <sub>12</sub> H <sub>34</sub> Cl <sub>6</sub> O <sub>14</sub> Tb <sub>2</sub>	C <sub>4</sub> H <sub>14</sub> N <sub>3</sub> O <sub>15</sub> Ce	C <sub>4</sub> H <sub>14</sub> N <sub>3</sub> O <sub>15</sub> Pr	C <sub>6</sub> H <sub>16</sub> N <sub>3</sub> O <sub>14</sub> Y	C <sub>6</sub> H <sub>16</sub> GdN <sub>3</sub> O <sub>14</sub>	C <sub>6</sub> H <sub>16</sub> N <sub>3</sub> TbO <sub>14</sub>
formula weight	932.93	484.30	485.09	443.13	511.47	513.14
T, K	173(2)	173(2)	173(2)	173(2)	173(2)	293(2)
cryst syst	triclinic	orthorhombic	orthorhombic	monoclinic	monoclinic	monoclinic
space group	<i>P</i> $\bar{1}$	<i>P</i> 2 <sub>1</sub> 2 <sub>1</sub> 2 <sub>1</sub>	<i>P</i> 2 <sub>1</sub> 2 <sub>1</sub> 2 <sub>1</sub>	<i>P</i> 2 <sub>1</sub> / <i>c</i>	<i>P</i> 2 <sub>1</sub> / <i>c</i>	<i>P</i> 2 <sub>1</sub> / <i>c</i>
<i>a</i> , Å	7.1120(14)	7.8685(16)	7.8595(16)	7.7827(16)	7.8146(16)	7.8085(16)
<i>b</i> , Å	8.7190(17)	13.304(3)	13.291(3)	12.816(3)	12.839(3)	12.923(3)
<i>c</i> , Å	12.492(3)	13.323(3)	13.327(3)	15.132(3)	15.207(3)	15.129(3)
$\alpha$ , deg	69.99(3)	90	90	90	90	90
$\beta$ , deg	76.44(3)	90	90	100.37(3)	100.68(3)	101.04(3)
$\gamma$ , deg	66.88(3)	90	90	90	90	90
<i>V</i> , Å <sup>3</sup>	664.9(2)	1394.7(5)	1392.1(5)	1484.6(5)	1499.4(5)	1498.4(5)
<i>Z</i>	1	4	4	4	4	4
<i>D</i> <sub>calcd</sub> , g cm <sup>-3</sup>	2.330	2.306	2.315	1.983	2.266	2.275
$\mu$ (Mo <i>K</i> $\alpha$ ), mm <sup>-1</sup>	5.938	3.356	3.592	4.013	4.507	4.803
<i>F</i> (000)	450	948	952	896	996	1000
crystal size (mm <sup>3</sup> )	0.200 × 0.120 × 0.071	0.260 × 0.210 × 0.112	0.350 × 0.330 × 0.150	0.300 × 0.250 × 0.130	0.201 × 0.112 × 0.053	0.30 × 0.20 × 0.15
$\theta$ range for data collection (°)	1.75 to 27.49	2.16 to 27.46	2.16 to 27.49	2.10 to 27.48	2.09 to 27.48	2.09 to 27.53
limiting indices	-9 ≤ <i>h</i> ≤ 9, -11 ≤ <i>k</i> ≤ 11, -16 ≤ <i>l</i> ≤ 16	-10 ≤ <i>h</i> ≤ 10, -17 ≤ <i>k</i> ≤ 17, -15 ≤ <i>l</i> ≤ 17	-10 ≤ <i>h</i> ≤ 10, -17 ≤ <i>k</i> ≤ 17, -17 ≤ <i>l</i> ≤ 15	-10 ≤ <i>h</i> ≤ 10, -15 ≤ <i>k</i> ≤ 16, -19 ≤ <i>l</i> ≤ 18	-10 ≤ <i>h</i> ≤ 10, -16 ≤ <i>k</i> ≤ 16, -13 ≤ <i>l</i> ≤ 19	-10 ≤ <i>h</i> ≤ 10, 0 ≤ <i>k</i> ≤ 16, 19 ≤ <i>l</i> ≤ 19
reflections collected/unique	5879/3033	12346/3178	12278/3186	12922/3398	7002/3401	5270/3243
<i>R</i> <sub>int</sub>	0.0226	0.0446	0.0591	0.0636	0.0364	0.1449
completeness to $\theta_{\max}$	99.0%	99.7%	99.9%	99.6%	99.0%	94.0%
absorption correction	semiempirical from equivalents	semiempirical from equivalents	semiempirical from equivalents	semiempirical from equivalents	semiempirical from equivalents	empirical
data/restraints/parameters	3033/15/187	3178/8/238	3186/11/239	3398/0/239	3401/8/239	3243/15/231
GOF on <i>F</i> <sup>2</sup>	1.245	1.083	1.080	1.323	1.115	1.005
<i>R</i> 1 [ <i>I</i> > 2 $\sigma$ ( <i>I</i> )]	0.0257	0.0199	0.0325	0.0577	0.0379	0.0902
<i>wR</i> 2 [ <i>I</i> > 2 $\sigma$ ( <i>I</i> )]	0.0783	0.0472	0.0713	0.1238	0.0809	0.2285
<i>R</i> 1 (all data)	0.0263	0.0200	0.0332	0.0669	0.0425	0.1079
<i>wR</i> 2 (all data)	0.0787	0.0473	0.0729	0.1392	0.0835	0.2395
largest diff. peak and hole (e <sup>-</sup> Å <sup>-3</sup> )	2.950 and -0.893	0.763 and -0.317	1.451 and -0.927	0.768 and -0.694	0.816 and -0.903	2.336 and -3.014

Figure 1. FTIR spectra of erythritol and its two metal complexes, TbE(I) and GdE in the 3800–2600 and 1700–650 cm<sup>-1</sup> region.

bands in the 1500–650  $\text{cm}^{-1}$  region. For the  $\text{GdCl}_3$ -erythritol complex, a similar IR spectrum can be obtained, which indicates that other lanthanide ions also can form the fifth coordination structure.

**Structure of  $\text{TbCl}_3$ -erythritol (TbE(I)).** The crystal structure of TbE(I) was shown in Figure 2. All H atoms are

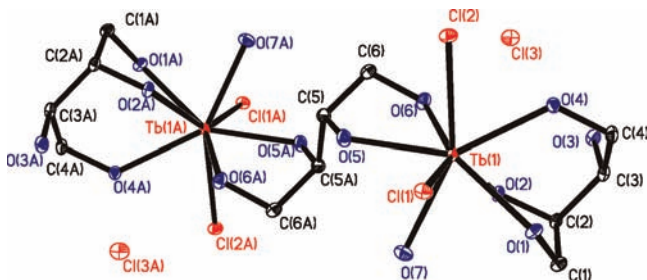


**Figure 2.** Crystal structure of TbE(I).

not shown here.  $\text{Tb}^{3+}$  is eight-coordinated to three hydroxyl groups (1, 2, and 4-OH) from one erythritol molecule, two chloride ions, one water molecule, and two hydroxyl groups from another erythritol molecule, so erythritol can be used as a two bidentate ligand or three hydroxyl group donor. Two coordination modes of erythritol coexist in the structure of TbE(I), which is consistent with the corresponding IR spectrum (more bands appear in the 1500–650  $\text{cm}^{-1}$  region). Tb–O distances are from 2.368 to 2.449 Å; Tb–Cl distances are 2.6750 and 2.6979 Å, respectively. The hydrogen bond data show that there are O–H...O and O–H...Cl hydrogen bonds in TbE(I). For the three hydroxyl group donor erythritol, its O3 does not coordinate to metal ions, but it can form a hydrogen bond with O5 via  $[x, y+1, z]$  symmetric operation (O5–H11...O3 distance is 2.652 Å, and the bond angle is 173.4°). Other hydrogen bonds belong to O–H...Cl hydrogen bonds. Cl3 does not coordinate to metal ions, and Cl3 can form hydrogen bonds with O6 (2.981 Å), O3 (3.094 Å), O2 (2.983 Å, via  $[-x+1, -y, -z+1]$  operation), O7 (3.102 Å, via  $[x+1, y, z]$  operation). For Cl1, O4–H10...Cl1 (3.197 Å, via  $[-x+1, -y+1, -z]$  operation) and O1–H7...Cl1 (3.068 Å, via  $[-x+2, -y+1, -z]$  operation) were observed. For Cl2, O7–H13...Cl2 (3.190 Å, via  $[x+1, y, z]$  operation) exists in the structure. For the coordinated water molecule, H13–O7–H14, hydrogen bonds are formed with Cl2 and Cl3. Therefore, extensive hydrogen bond networks have formed in TbE(I).

The C–O bond lengths are 1.345–1.458 Å, C–C bond lengths are 1.400–1.530 Å, O–C–C bond angles are 105.6–118.8°, and C–C–C bond angles are 114.0–116.5°. The C–C bond length is 1.51 Å, C–O bond lengths are 1.39 and 1.47 Å, O–C–C bond angle is 107°, and C–C–C bond angle is 113° for erythritol itself.<sup>49</sup> Compared with erythritol itself, after complexation the three hydroxyl group donor erythritol is not symmetric. For TbE(I), the O–C–C bond angles are 106.6°, 106.9°, 109.5°, 112.1°, 108.7°, 110.7°, 104.5°, 109.9°, and 105.0°; the bond angle of C(6)–C(5)–C(5)#1 is 114.2°, bond angle of C(1)–C(2)–C(3) is 114.4°, and bond angle of C(4)–C(3)–C(2) is 115.8°, respectively, which indicates the coordination of metal ions. Because O3 does not coordinate to a metal ion, the torsion angle of C(1)–C(2)–C(3)–O(3) is –177.6°, close to –180°, and the torsion angle of C(1)–C(2)–C(3)–C(4) is –50.4°.

For lanthanide chloride-erythritol complexes, four coordination structures have been observed in the references.<sup>40–45</sup> The first coordination mode is that the  $\text{Ln}^{3+}$  ion coordinates with four hydroxyl groups from two erythritol molecules, four water molecules, and one chloride ion, the coordination number is 9, and the formula is  $\text{LnCl}_3 \cdot \text{C}_4\text{H}_{10}\text{O}_4 \cdot 6\text{H}_2\text{O}$ , including  $\text{LaCl}_3$ ,  $\text{PrCl}_3$ ,  $\text{NdCl}_3$ ,  $\text{EuCl}_3$ , and  $\text{TbCl}_3$ -erythritol complexes.<sup>40</sup> The second one was observed in the europium chloride-erythritol complex ( $2\text{EuCl}_3 \cdot 2\text{C}_4\text{H}_{10}\text{O}_4 \cdot 7\text{H}_2\text{O}$ ); its characteristic is the presence of binuclear europium ions with different coordination structures: one  $\text{Eu}^{3+}$  ion is 9-coordinated with five Eu–O bonds from water molecules and four from hydroxyl groups of two erythritol molecules, and another  $\text{Eu}^{3+}$  is eight-coordinated with two water molecules, two chloride ions, and four hydroxyl groups from two erythritol molecules.<sup>41</sup> The third one is  $\text{NdCl}_3 \cdot 2.5\text{C}_4\text{H}_{10}\text{O}_4 \cdot \text{C}_2\text{H}_5\text{OH}$ ;  $\text{Nd}^{3+}$  is nine-coordinated to eight hydroxyl groups from three erythritol molecules and one chloride ion.<sup>42</sup> The fourth structure is  $\text{ErE}$  ( $\text{ErCl}_2 \cdot \text{C}_4\text{H}_9\text{O}_4 \cdot 2\text{C}_2\text{H}_5\text{OH}$ );  $\text{Er}^{3+}$  is eight-coordinated with three hydroxyl groups of one erythritol molecule, two hydroxyl groups from another erythritol molecule, two ethanol molecules, and one chloride. For one erythritol molecule, it provides three hydroxyl groups to one erbium ion and two hydroxyl groups to another erbium ion. Among them, one hydroxyl group is coordinated to two metal ions, which loses its hydrogen atom and becomes an oxygen bridge. Therefore, erythritol becomes  $\text{C}_4\text{H}_9\text{O}_4$ .<sup>43</sup> Here, the fifth structure (TbE(I)) has been obtained. For such a simple molecule, five topological structures can be observed, which indicate the complexity of the interactions between lanthanide ions and carbohydrates.

For alkaline-earth metal ion, three calcium chloride-erythritol complexes have been obtained.<sup>40</sup> For transition metal ions, two  $\text{CuCl}_2$ -erythritol complexes were observed.<sup>45</sup> Here, for lanthanide chloride-erythritol complexes, five coordination structures have been observed, which indicate that the interactions between lanthanide and erythritol are more complicated. Compared to  $\text{Ca}^{2+}$  or  $\text{Cu}^{2+}$ , lanthanide ions often have high coordination number (8 or 9 here), several hydroxyl groups are coordinated to metal ions, and more extensive hydrogen bond networks can be obtained in the lanthanide complexes.

**Structures of Lanthanide Nitrate-Erythritol Complexes.** The FTIR spectra of PrEN, CeEN, YEN, GdEN, and TbEN were shown in Figure 3. The IR bands and possible assignment were listed in Table 2. Their spectra belong to two kinds of structures: one is water-involved and the other one does not have water. The structures of PrEN and CeEN having water molecules are newly observed. The FTIR spectra of YEN, TbEN, and GdEN are similar to the spectra of NdEN and EuEN, whose structures were determined.<sup>40,44</sup>

PrEN and CeEN have very similar IR spectra, which indicate that they should have similar structures. The obvious characteristic of their IR spectra is that there is  $\delta\text{H}_2\text{O}$  located at 1633  $\text{cm}^{-1}$ , which indicate the existence of water molecules in PrEN and CeEN. The  $\nu\text{OH}$  vibrations are located at 3573 and 3333  $\text{cm}^{-1}$  for PrEN and 3571 and 3331  $\text{cm}^{-1}$  for CeEN, which are related to hydrogen bond networks in their structures, including weak hydrogen bond and relatively stronger hydrogen bonds, respectively. One of the  $\nu\text{OH}$  bands is located at  $\sim 3571 \text{ cm}^{-1}$ , which indicates that there may be an uncoordinated hydroxyl group.  $\nu\text{CH}$  vibrations are weak bands, which is similar to other metal-sugar complexes. Most of the bands in the 1500–1250  $\text{cm}^{-1}$  region are related to

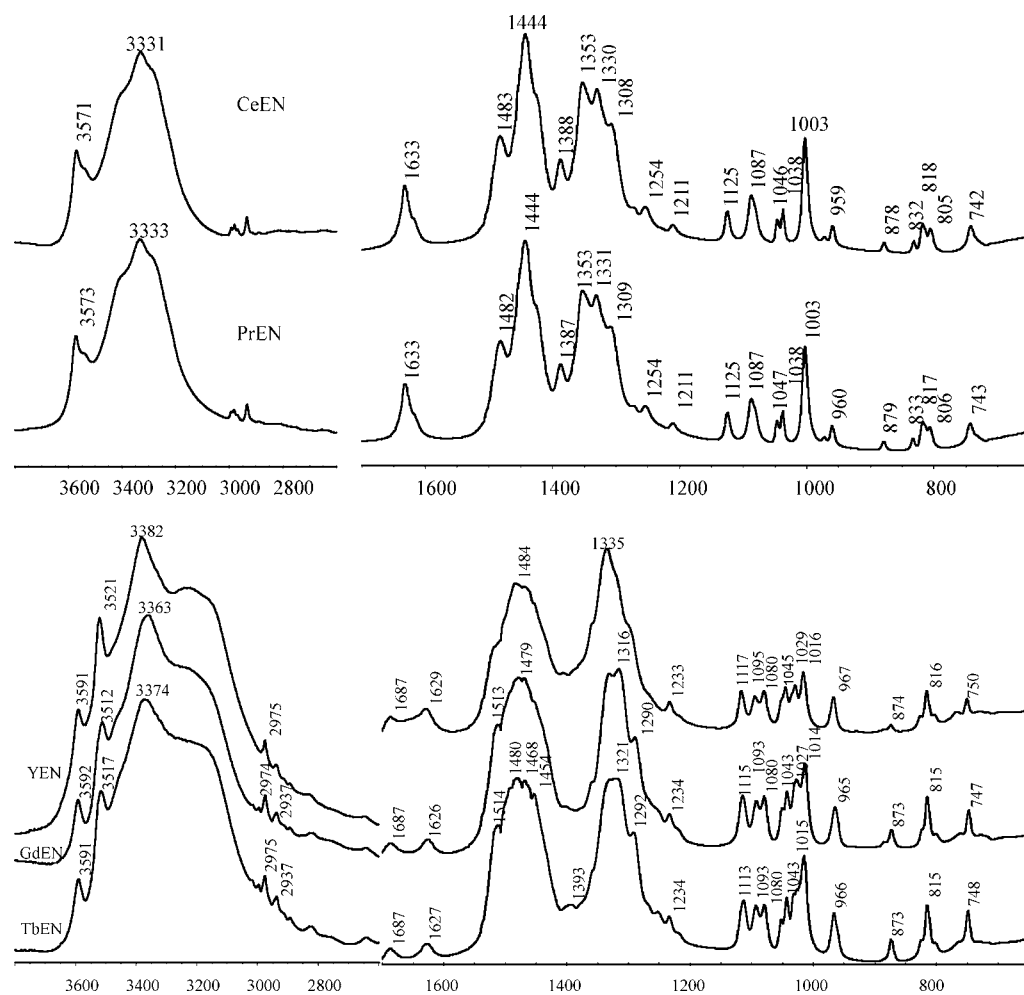


Figure 3. FTIR spectra of lanthanide nitrate-erythritol complexes, PrEN, CeEN, YEN, GdEN, and TbEN.

nitrate ions. Here, all three nitrate ions are coordinated to metal ions, and the bands at  $\sim 1483$ ,  $1444$ , and  $1388\text{ cm}^{-1}$  may be related to  $\nu\text{as}(\text{NO}_2)$  and  $\delta\text{CH}_2$  and the bands at  $\sim 1353$ ,  $1330$ , and  $1308\text{ cm}^{-1}$  may be related to  $\nu\text{s}(\text{NO}_2)$ .<sup>50</sup> The bands in the  $1250\text{--}850\text{ cm}^{-1}$  region related to  $\nu\text{CO}$ ,  $\nu\text{CC}$ ,  $\delta\text{COH}$ ,  $\delta\text{CCH}$ , and  $\nu\text{NO}$  also shifted compared to erythritol, which shows the coordination of hydroxyl groups to metal ions. Also, the bands are not complicated such as in TbE(I), which indicates that maybe only one coordination mode appears for erythritol.

For three structures without water, YEN, GdEN, and TbEN, the  $\nu\text{OH}$  bands in the salt spectra were broadened. The bands at  $3591$ ,  $3521$ , and  $3382\text{ cm}^{-1}$  for YEN,  $3591$ ,  $3517$ , and  $3374\text{ cm}^{-1}$  for TbEN and  $3592$ ,  $3512$ , and  $3363\text{ cm}^{-1}$  for GdEN were observed. The OH stretching vibrations can be assigned to the H-bonds formed between the hydroxyl groups and nitrate ions. The existence of the bands at  $\sim 3590$  and  $\sim 3517\text{ cm}^{-1}$  indicates that there may have been uncoordinated hydroxyl groups. The free erythritol exhibited four bands at  $2971$ ,  $2957$ ,  $2928$ , and  $2911\text{ cm}^{-1}$  assigned to the stretch vibrations of the CH group ( $\nu\text{CH}$ ). The bands shifted in the three complexes and the intensities became weaker upon coordination (Figure 3). For the three metal complexes, the peak positions of  $\nu\text{CH}$  are similar. The intensity of  $\nu\text{CH}$  is decreased and the vibrations of OH have masked the CH bands.

The bands at  $\sim 1687$  and  $\sim 1627\text{ cm}^{-1}$  are related to deformation of COH (uncoordinated OH). In the  $1550\text{--}1200\text{ cm}^{-1}$  region, the bands located at  $1484$ ,  $1464$ , and  $1455\text{ cm}^{-1}$  for YEN;  $1513$ ,  $1479$ , and  $1472\text{ cm}^{-1}$  for GdEN; and  $1514$ ,  $1480$ ,  $1468$ , and  $1454\text{ cm}^{-1}$  for TbEN may be related to  $\nu\text{asNO}_2$  and  $\delta\text{CH}_2$ . In addition,  $1335$  and  $1299\text{ cm}^{-1}$  for YEN;  $1332$ ,  $1316$ , and  $1290\text{ cm}^{-1}$  for GdEN; and  $1329$ ,  $1321$ , and  $1292\text{ cm}^{-1}$  for TbEN may be related to  $\nu\text{sNO}_2$ .<sup>48,50</sup> The bands split into several bands after complexation, indicating the coordination of nitrate ions and the decrease of nitrate ion symmetry. The peak positions are similar for the three compounds, but different with metal nitrates. The changes of the bands have reflected the coordination of nitrate ions, and three similar spectra indicate that three compounds have the same structures.

The bands in the  $1250\text{--}850\text{ cm}^{-1}$  region may be assigned mainly to CO, CC, COH, CCH, and CCO vibrations of erythritol and N–O vibrations of nitrate ions.<sup>48,50</sup> The changes of these bands also indicate the formation of lanthanide nitrate-erythritol complexes. Especially for the stronger bands in the region,  $1081$  and  $1055\text{ cm}^{-1}$  bands for erythritol itself assigned mainly to C–O stretching vibrations<sup>48,50</sup> are shifted to  $1080$ ,  $1052$ ,  $1043$ , and  $1015\text{ cm}^{-1}$  for TbEN;  $1080$ ,  $1051$ ,  $1043$ ,  $1027$ , and  $1014\text{ cm}^{-1}$  for GdEN; and  $1080$ ,  $1045$ ,  $1029$ , and  $1016\text{ cm}^{-1}$  for YEN, respectively, which indicates the coordination of hydroxyl

Table 2. IR Bands, FIR, THz Spectral Data, and Possible Assignments for Lanthanide Nitrate-Erythritol Complexes<sup>a</sup>

E	PrEN	CeEN	YEN	GdEN	TbEN	possible assignments <sup>48,50–57</sup>	E	PrEN	CeEN	YEN	GdEN	TbEN	possible assignments <sup>48,50–57</sup>
	3573	3571	3591	3592	3591	$\nu$ OH	1055				1051	1052	
			3521	3512	3517	$\nu$ OH		1047	1046	1045	1043	1043	$\nu$ CO(2), $\nu$ CO(3), $\nu$ CO(1), $\nu$ CO(4), $\delta$ CO(1)H, $\delta$ CO(4)H
3271	3333	3331	3382	3363	3374	$\nu$ OH							
3263						$\nu$ OH		1038	1038	1029	1027		$\nu$ CO, $\nu$ NO
3251						$\nu$ OH		1003	1003	1016	1014	1015	$\nu$ CO, $\nu$ NO
3238						$\nu$ OH							
2971			2975	2974	2975	$\nu$ asC(1)H <sub>2</sub> , $\nu$ asC(4)H <sub>2</sub>	968	960	959	967	965	966	$\rho$ C(1)H <sub>2</sub> , $\rho$ C(4)H <sub>2</sub>
2957				2937	2937		918						
2928						$\nu$ C(2)H, $\nu$ C(3)H	884	879	878	874	873	873	$\nu$ CC, $\rho$ C(1)H <sub>2</sub> , $\rho$ C(4)H <sub>2</sub>
2911						$\nu$ sC(1)H <sub>2</sub> , $\nu$ sC(4)H <sub>2</sub>	865	833	832				
2820								817	818	816	815	815	$\gamma$ NO <sub>2</sub>
2717								806	805				
2663							710	743	742	750	747	748	$\tau$ OH <sub>inter</sub> , $\delta$ NO <sub>2</sub>
			1687	1687	1687	$\delta$ COH	694						
	1633	1633				$\delta$ H <sub>2</sub> O	616			635	616	608	$\delta$ CCO
			1629	1626	1627	$\delta$ COH		534	526	544	539	536	
				1513	1514	$\nu$ asNO <sub>2</sub>	488		498		433		$\tau$ O(1)H, $\tau$ O(4)H
	1482	1483	1484	1479	1480	$\nu$ as(NO <sub>2</sub> ), $\delta$ CH <sub>2</sub>	429			395	398	393	$\tau$ O(1)H, $\tau$ O(4)H
1457			1464	1472	1468	$\delta$ C(1)H <sub>2</sub> , $\delta$ C(4)H <sub>2</sub>	421						
1417	1444	1444	1455		1454	$\nu$ as(NO <sub>2</sub> ), $\omega$ C(1)H <sub>2</sub> , $\omega$ C(4)H <sub>2</sub> , $\delta$ CO(1)H, $\delta$ CO(4)H	378	367	364	375	372	371	$\nu$ MO
								341	339	330	325	330	$\nu$ MO
	1387	1388			1393	$\nu$ as(NO <sub>2</sub> )	299	293	295	309	303	309	$\nu$ MO
1366	1353	1353				$\nu$ s(NO <sub>2</sub> ), $\gamma$ C(2)H, $\gamma$ C(3)H, $\delta$ CO(2)H, $\delta$ CO(3)H	274	269	267		271	269	$\nu$ MO
							240			238	231	221	$\nu$ MO
	1331	1330	1335	1332	1329	$\nu$ s(NO <sub>2</sub> ), $\delta$ CO(1)H, $\delta$ CO(4)H, $\delta$ CCH	188	183	180	199	189	177	$\nu$ MO
							172			165			$\nu$ MO, $\delta$ OMO
				1316	1321	$\nu$ s(NO <sub>2</sub> )	150						
1308	1309	1308	1299	1290	1292	$\nu$ s(NO <sub>2</sub> )	137	137	137	137		129	$\nu$ MO
1272						$\delta$ CCH	105	105	105	105	101	100	
1256	1254	1254	1233	1234	1234	$\tau$ wC(1)H <sub>2</sub> , $\tau$ wC(4)H <sub>2</sub> , $\delta$ CCH, $\delta$ COH		76	75	80	80	74	crystal lattice vibration, hydrogen bonds
1217	1211	1211				$\delta$ CO(2)H, $\delta$ CO(3)H, $\delta$ CO(1)H, $\delta$ CO(4)H, $\gamma$ C(2)H, $\gamma$ C(3)H	67	60	59	67		54	
							70	74	74	77	72	73	crystal lattice vibration, hydrogen bonds
	1125	1125	1117	1115	1113		64			66		63	
			1095	1093	1093		61	59	59	59	55	53	
1081	1087	1087	1080	1080	1080	$\nu$ CO(2), $\nu$ CO(3), $\nu$ CO(1), $\nu$ CO(4)		35	35		45	45	

<sup>a</sup>Abbreviations:  $\nu$ , stretching;  $\delta$ , in-plane bending;  $\gamma$ , out-of-plane bending;  $\omega$ , wagging;  $\rho$ , rocking;  $\tau$ , torsion; s, symmetric; as, asymmetric.

groups to metal ions. More bands appear in this region, which shows the change of the conformation of erythritol, the decrease of its symmetry. The band at 1015 cm<sup>-1</sup> in TbEN, 1014 cm<sup>-1</sup> in GdEN, and 1016 cm<sup>-1</sup> in YEN becomes the strongest peak in the region. The 968 cm<sup>-1</sup> band for erythritol itself is shifted to 966, 965, or 967 cm<sup>-1</sup> for TbEN, GdEN, and YEN, respectively.

Although the coordination mode of erythritol is the same for the metal complexes with and without water (coordination with 1, 2, and 3-OH), their IR spectra in the 1500–650 cm<sup>-1</sup> region are different, maybe because the changes of conformation of erythritol induced by complexation are various. The IR results indicate that the hydroxyl groups of erythritol and nitrate ions took part in the metal-carbohydrate interaction and there may have one uncoordinated hydroxyl group; the hydrogen-bond network rearranged upon sugar metalation; the conformation of erythritol skeleton changed as a result of salt formation. From the similarity of FTIR spectra of YEN, TbEN, GdEN, EuEN, and NdEN, the coordination structures of Y, Gd, and Tb-complexes can be deduced from the structures of NdEN and EuEN:<sup>40,44</sup> Y<sup>3+</sup>,

Tb<sup>3+</sup>, or Gd<sup>3+</sup> is also ten-coordinated with three hydroxyl groups from one erythritol molecule, three bidentate nitrate ions, and one ethanol molecule. Different lanthanide ions can form similar complexes with a ligand.

**Crystal Structures of Lanthanide Nitrate-Erythritol Complexes.** The crystal structures of CeEN (Ce(NO<sub>3</sub>)<sub>3</sub>·C<sub>4</sub>H<sub>10</sub>O<sub>4</sub>·2H<sub>2</sub>O) and TbEN (Tb(NO<sub>3</sub>)<sub>3</sub>·C<sub>4</sub>H<sub>10</sub>O<sub>4</sub>·C<sub>2</sub>H<sub>5</sub>OH) shown in Figure 4 represented the structures with water and without water, respectively. For PrEN and CeEN, Ln<sup>3+</sup> is 11-coordinated to three hydroxyl groups from one erythritol molecule, six oxygen atoms from three nitrate ions, and two water molecules. Ce–O distances are from 2.493 to 2.824 Å, and Pr–O distances from 2.476 to 2.830 Å, respectively. According to the hydrogen bonds data, there are O–H···O and O–H···N hydrogen bonds. Hydroxyl groups of erythritol form hydrogen bonds with oxygen atoms of nitrate ions and hydroxyl group of erythritol; coordinated water molecules form hydrogen bonds with oxygen and N atoms of nitrate ions and hydroxyl group of erythritol. For uncoordinated hydroxyl group of erythritol, O4, hydrogen bonds are formed with the hydroxyl group of erythritol, coordinated

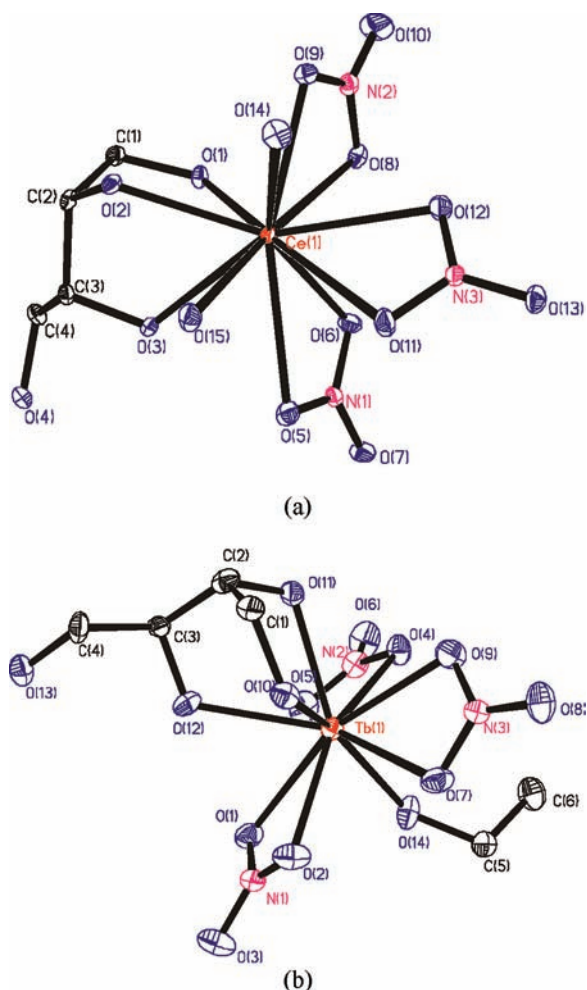


**Figure 4.** Crystal structures of CeEN and TbEN: (a) The structure and atom numbering scheme of  $\text{Ce}(\text{NO}_3)_3 \cdot \text{C}_4\text{H}_{10}\text{O}_4 \cdot 2\text{H}_2\text{O}$ ; (b) the structure and atom numbering scheme of  $\text{Tb}(\text{NO}_3)_3 \cdot \text{C}_4\text{H}_{10}\text{O}_4 \cdot \text{C}_2\text{H}_5\text{OH}$ .

water, and O and N atoms of nitrate ion (O1–H8...O4, 2.739 Å, via  $[x-1/2, -y+3/2, -z+2]$  operation, O15–H14...O4, 2.854 Å, via  $[-x+1/2, -y+2, z-1/2]$  operation, O4–H7...O10, 2.796 Å, via  $[x+1, y, z]$  operation, O4–H7...N2, 3.537 Å, via  $[x+1, y, z]$  operation). Compared with erythritol, the bond angle of C(1)–C(2)–C(3) is  $115.1^\circ$  in PrEN and  $115.3^\circ$  in CeEN; and C(4)–C(3)–C(2) is  $112.8^\circ$  in PrEN and  $112.3^\circ$  in CeEN, respectively, which reflects the changes of the conformation of erythritol.

For  $\text{Tb}(\text{NO}_3)_3 \cdot \text{C}_4\text{H}_{10}\text{O}_4 \cdot \text{C}_2\text{H}_5\text{OH}$ , the ten-coordinated  $\text{Tb}^{3+}$  binds to three hydroxyl groups of one erythritol molecule, three bidentate nitrate ions, and one ethanol molecule. YEN and GdEN have the same structures as TbEN. The crystal structures confirm previous IR results. Y–O distances are from 2.358 to 2.594 Å; Gd–O distances are from 2.398 to 2.596 Å; and Tb–O distances are from 2.373 to 2.581 Å, respectively. By comparison of the coordination number and M–O bond distances in TbE and TbEN,  $\text{Tb}^{3+}$  is 8-coordinated and Tb–O distances are from 2.368 to 2.449 Å in TbE and  $\text{Tb}^{3+}$  is 10-coordinated and Tb–O distances are from 2.373 to 2.581 Å. The results indicate that, when the coordination number is higher, the M–O distances are longer. In the references, La–O distances are from 2.531 to 2.925 Å in  $2\text{La}(\text{NO}_3)_3 \cdot \text{C}_4\text{H}_{10}\text{O}_4 \cdot 8\text{H}_2\text{O}$ ,<sup>43</sup>

Eu–O distances are from 2.421 to 2.600 Å in  $\text{Eu}(\text{NO}_3)_3 \cdot \text{C}_4\text{H}_{10}\text{O}_4 \cdot \text{C}_2\text{H}_5\text{OH}$ ,<sup>44</sup> and Nd–O distances are from 2.455 to 2.620 Å in  $\text{Nd}(\text{NO}_3)_3 \cdot \text{C}_4\text{H}_{10}\text{O}_4 \cdot \text{C}_2\text{H}_5\text{OH}$ .<sup>40</sup> The Ln–O bond distances have small differences and the changes of Ln–O distances are consistent with lanthanide contraction.

Erythritol is not symmetric after complexation with  $\text{Y}^{3+}$ ,  $\text{Gd}^{3+}$ , and  $\text{Tb}^{3+}$  ions. The coordination of metal ion has influence on the conformation of erythritol; for example, for the ligand erythritol, C–C–C bond angle is  $112.9^\circ$ ;<sup>49</sup> after complexation, the angles become  $118.4^\circ$  and  $111.4^\circ$  in TbEN,  $116.8^\circ$  and  $113.0^\circ$  in GdEN, and  $116.3^\circ$  and  $112.8^\circ$  in YEN. The angles are  $116.5^\circ$  and  $113.0^\circ$  in NdEN, and  $116.6^\circ$  and  $113.7^\circ$  in EuEN, respectively. The results show that the changes of the conformation of erythritol induced by the coordination of different lanthanide ions have little difference. La ion is 11-coordinated and it has larger differences compared with other lanthanide ions in  $2\text{La}(\text{NO}_3)_3 \cdot \text{C}_4\text{H}_{10}\text{O}_4 \cdot 8\text{H}_2\text{O}$ .

**FIR and THz Spectra of the Lanthanide-Erythritol Complexes.** FIR and THz are effective methods to determine the formation of metal–ligand complexes.<sup>54–57</sup> The FIR and THz spectra of erythritol and these lanthanide–erythritol complexes are shown in Figures 5 and 6. The corresponding band positions of lanthanide nitrate–erythritol complexes are listed in Table 2. As shown in the figures, in the  $650\text{--}50\text{ cm}^{-1}$  region the bands of TbE(I) are located at 527, 479, 414, 393, 350, 285, 245, 218, 203, 177, 136, and  $102\text{ cm}^{-1}$ . After complexation with Tb ion, new bands are observed compared to erythritol; most of them are related to Tb–O vibrations.  $\text{Tb}^{3+}$  is nine-coordinated in TbE(I). Each M–O is located in different environment, so several bands can be observed and some bands masked for the degeneration. The bands near  $200\text{ cm}^{-1}$  are usually regarded as M–O vibrations for metal–sugar complexes;<sup>54</sup> therefore, the bands at 245, 218, 203, and  $177\text{ cm}^{-1}$  for TbE(I) belong to M–O vibrations. 136 and  $102\text{ cm}^{-1}$  bands may be related to Tb–Cl vibrations. Other bands may be related to M–O–H, M–O–C, or O–M–O deformation. Also, the peak positions and relative intensities of the bands in TbE(I) are changed compared to erythritol itself.

For PrEN and CeEN, the bands at 183 and  $180\text{ cm}^{-1}$  can be assigned to M–O vibrations. The bands are diffused for PrEN because of the influence of water. PrEN and CeEN have similar FIR spectra, which indicate that they should have the same coordination structures. For three metal complexes without water, they have more than ten bands in the region as shown in Figure 5. The three FIR spectra are similar in peak position and relative intensities because of the similarity of their structures. The bands at 269, 221, 177, and  $129\text{ cm}^{-1}$  for TbEN; 231 and  $189\text{ cm}^{-1}$  for GdEN; and 238 and  $199\text{ cm}^{-1}$  for YEN may be related to M–O vibrations. Other bands in the region may be related to M–O vibration and deformation of OMO.<sup>48,50</sup> Also, the bands of YEN, TbEN, and GdEN in this region are different from those of erythritol itself, which confirms the formation of metal complexes.

Considering that some M–O vibrations are related to oxygen atoms of nitrate ions, we compared the Fourier self-deconvolution (FSD) results of TbE with TbEN. The FSD results are consistent with second derivative results. Many bands appear in their FSD results, which are related to each M–O vibration. Compared the two FSD spectra, 368, 328, 307,

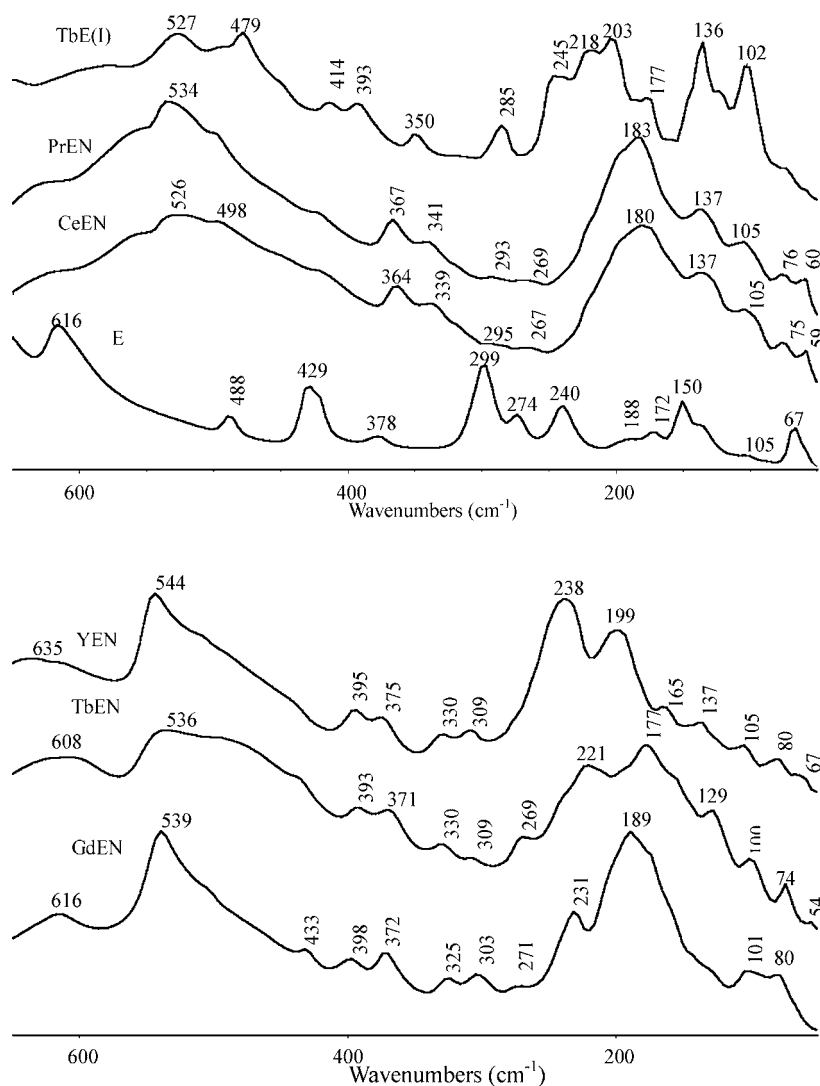


**Figure 5.** FIR spectra of erythritol and lanthanide-erythritol complexes in the 650–50 cm<sup>-1</sup> region.

and 269 cm<sup>-1</sup> bands may be related oxygen atoms of nitrate ions in the 400–100 cm<sup>-1</sup> region.

The THz absorption bands of TbE(I) are located at 1.78 and 2.14 THz. For PrEN and CeEN having similar structures; the two compounds also have similar THz bands: 1.05, 1.78, and 2.22 THz for PrEN and 1.06, 1.76, and 2.23 THz for CeEN were observed, and the two spectra are different from those of erythritol itself.<sup>57</sup> Also, 1.76, 1.99, and 2.31 THz for YEN; 1.35, 1.64, and 2.17 THz for GdEN; and 1.35, 1.60, 1.88, and 2.19 THz for TbEN were observed for three compounds without water. The FIR and THz spectra confirm the formation of these metal complexes and show that YEN, TbEN, and GdEN have similar structures, and PrEN and CeEN have the same structure.

To clarify the bands in the THz region, second derivatives were performed using *Omicron 5.0* software for the THz spectrum of each sample, and the results show that the main bands and some relatively minor bands were emphasized in the second derivatives results in the 87–7 cm<sup>-1</sup> region. The main bands were observed for each sample, which has good agreement with the corresponding THz absorption spectrum. For TbE(I), the main bands at 59, 71, and 80 cm<sup>-1</sup> were observed; the bands at 21, 49, and 54 cm<sup>-1</sup> also can be

observed in the second derivative results. For CeEN, main bands are observed. For PrEN, the bands at 35, 59, and 74 cm<sup>-1</sup> are also observed, and the band at 74 cm<sup>-1</sup> has three child bands located at 70, 74, and 78 cm<sup>-1</sup>. For YEN, the bands at 21, 27, and 45 cm<sup>-1</sup> are weak peaks in the THz spectrum, but they are emphasized in the second derivative results. For GdEN, except for 45, 55, 72, and 80 cm<sup>-1</sup> bands observed in the THz absorption spectrum, the band at 64 cm<sup>-1</sup> is emphasized in the second derivatives results. For TbEN, the main bands at 45, 53, 63, and 73 cm<sup>-1</sup> are observed, and a weak band at 81 cm<sup>-1</sup> also can be identified. The results show that second derivative methods help with observing the THz bands. These bands in the THz region are related to crystal lattice vibration and hydrogen bonds, and so forth. For these metal complexes, the bands become broader compared to erythritol, maybe because after complexation the coordination structures have formed complicated, extensive hydrogen bond networks and some of them may be similar, so the bands become broader.

**Luminescence Spectra of TbE(I) and TbEN.** The luminescence spectra of TbE(I) and TbEN are shown in Figure 7, including their excitation and emission spectra. Here, terbium ion shows its characteristic emission spectrum in



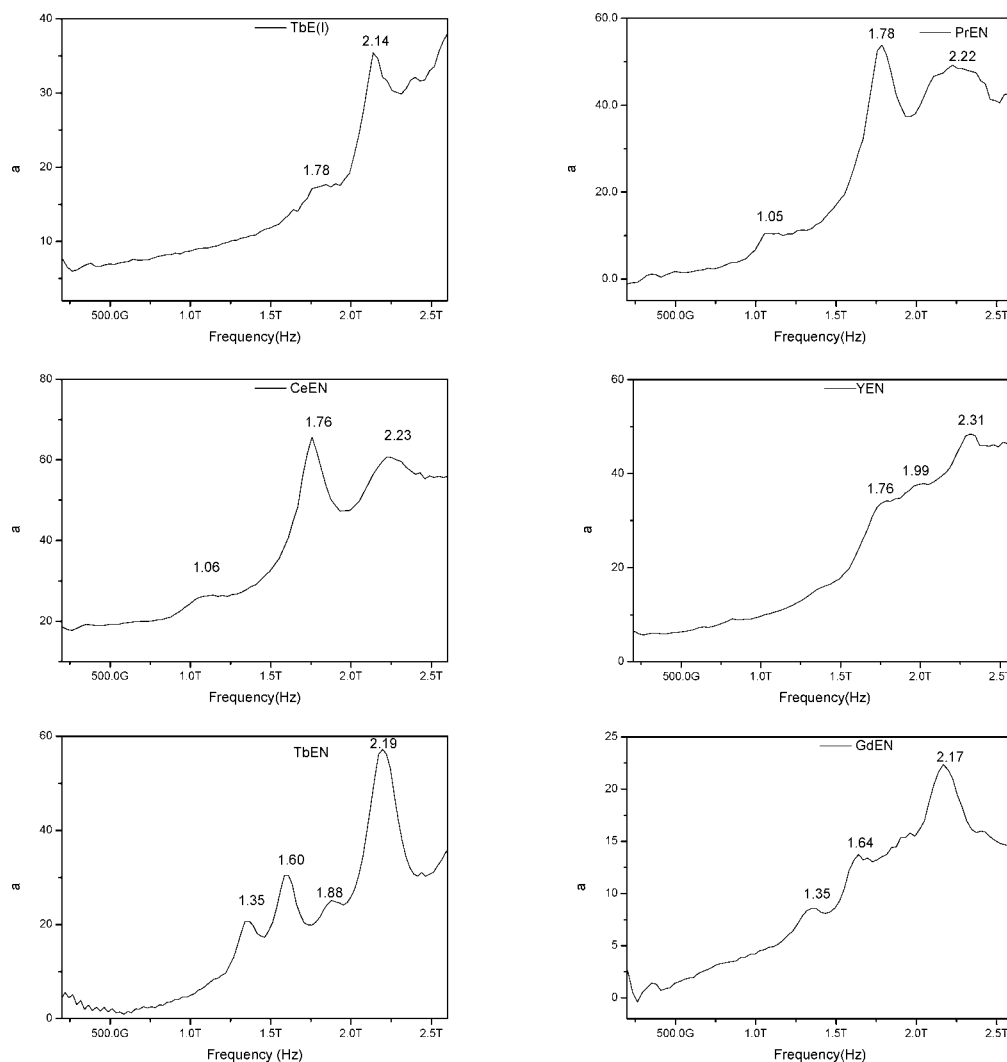


**Figure 6.** THz spectra of these metal complexes.

TbE(I) and TbEN. The assignments of the peaks in the emission spectrum of TbE(I) and TbEN are as follows:  $\sim 490$  nm ( $^5D_4 \rightarrow ^7F_6$ ),  $\sim 542$  and  $546$  nm ( $^5D_4 \rightarrow ^7F_5$ ),  $\sim 585$  nm ( $^5D_4 \rightarrow ^7F_4$ ),  $\sim 621$  nm ( $^5D_0 \rightarrow ^7F_3$ ).<sup>58</sup> The 583 nm band has a shoulder peak in TbE(I). The 544 nm band splits into 542 and 546 nm peaks in TbEN because  $Tb^{3+}$  is located at an asymmetric ligand field. Two  $Tb^{3+}$  ions have similar emission spectra, but the relative intensities of the peaks have some differences, which show that transition probability changes and reflects the influence of a different coordination sphere. Their excitation spectra are also similar to some extent; for example, 319, 340, 351, 368, and 376 nm bands can be observed for TbE, and TbEN has the similar band positions at 318, 341, 353, 369, and 380 nm. The similarity may be because they have the same ligand. The results indicate that lanthanide-erythritol complexes have characteristic luminescence properties of lanthanide ions, but their luminescence intensities are weaker than some lanthanide chelates, for example, several  $TbCl_3$ -carboxylic acid complexes.<sup>59</sup>

Based on above experimental results and the references, four coordination modes of erythritol have been observed as shown in Figure 8. To compare the coordination of different metal ions, the topological coordination structures of the metal complexes are listed in Table 3. The results

indicate that lanthanide ions often have higher coordination numbers, and for  $Ca^{2+}$  and  $Cu^{2+}$ , erythritol has two bidentate ligands or can be uncoordinated, but for lanthanide ions, different coordination modes of erythritol can be observed, which make the topological structures complicated. The differences in coordination modes of erythritol may be related to the charge and radius of metal ions. Erythritol is a relatively simple ligand. Lanthanide ions have high coordination number, so they can accept three hydroxyl groups from one erythritol in their coordination sphere.

Compared to another ligand, galactitol, it coordinates to lanthanide ions as two three-hydroxyl-group donors, but it has two coordination modes with alkaline-earth metal ions.<sup>25–29</sup> For example, for  $Ca^{2+}$ , one metal ion coordinates to one or two hydroxyl groups of one ligand. Galactitol has six hydroxyl groups, which results in the complicated coordination between galactitol and alkaline-earth metal ions. The coordination difference between erythritol and galactitol (erythritol has several coordination modes with lanthanide ions; galactitol has two coordination modes with alkaline-earth metal ions) are from the different chain and various metal ions.

When comparing lanthanide chloride and nitrate-erythritol complexes, lanthanide nitrate-erythritol complexes often have

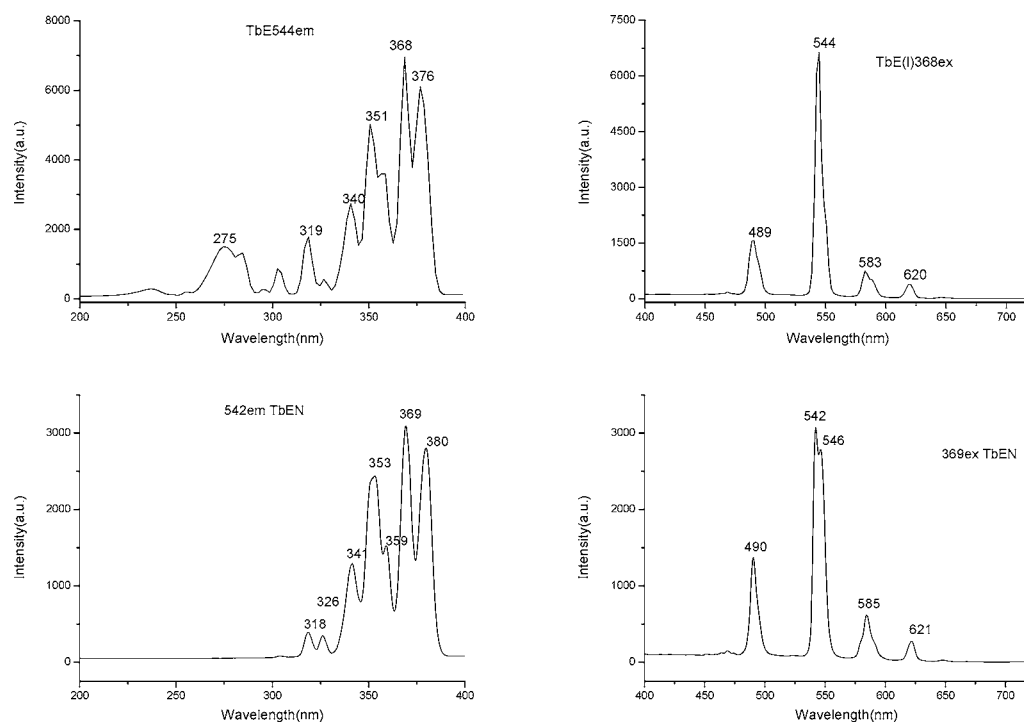


Figure 7. Luminescence spectra of TbE(I) and TbEN.

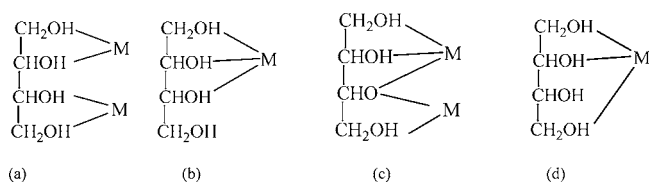


Figure 8. Four coordination modes of erythritol with metal ions.

higher coordination number (10 or 11 here) than lanthanide chloride-erythritol complexes because  $\text{NO}_3^-$  ions are used as bidentate ligands. There are three chloride ions: they can coordinate to metal ions or be hydrogen bonded. For three

nitrate ions, they are coordinated to metal ions, which make the coordination number high. For ZnEN, nitrate ions are monodentate ligands. For galactitol, nitrate ions can coordinate to metal ions or hydrogen bond; even all three nitrate ions may be hydrogen-bonded.<sup>60</sup> The results show that different ligands have various coordination modes; the ligand (erythritol), solvent (water or ethanol), and anions ( $\text{Cl}^-$  or  $\text{NO}_3^-$ ) are competitively coordinated to metal ions, which makes the interactions between metal ions and carbohydrates complicated. At the same time, extensive hydrogen bond networks form and the metal complexes have various structures.

Table 3. Summary of the Coordination Modes of the Metal-Erythritol Complexes<sup>a</sup>

stoichiometry	examples	C. N.	space group	OH	coordination mode of erythritol	H <sub>2</sub> O	ethanol	Cl <sup>-</sup>	NO <sub>3</sub> <sup>-</sup>
2CaCl <sub>2</sub> ·C <sub>4</sub> H <sub>10</sub> O <sub>4</sub> ·4H <sub>2</sub> O	CaE(I)	7	P2 <sub>1</sub> /c	2	a	2		3 <sup>a</sup>	
CaCl <sub>2</sub> ·C <sub>4</sub> H <sub>10</sub> O <sub>4</sub> ·4H <sub>2</sub> O	CaE(II)	8	C2/c	4	a	4		0	
CaCl <sub>2</sub> ·2C <sub>4</sub> H <sub>10</sub> O <sub>4</sub> ·4H <sub>2</sub> O	CaE(III)	8	Fddd	8	a	0		0	
MCl <sub>2</sub> ·C <sub>4</sub> H <sub>10</sub> O <sub>4</sub>	CuE(I), MnE	6	C2/c	4	a	0		2	
CuCl <sub>2</sub> ·C <sub>4</sub> H <sub>10</sub> O <sub>4</sub>	CuE(II)	4	P $\bar{1}$	2	a and uncoordinated	0		2	
LnCl <sub>3</sub> ·C <sub>4</sub> H <sub>10</sub> O <sub>4</sub> ·6H <sub>2</sub> O	PrE, NdE	9	P $\bar{1}$	4	a	4		1	
ErCl <sub>3</sub> ·C <sub>4</sub> H <sub>10</sub> O <sub>4</sub> ·2C <sub>2</sub> H <sub>5</sub> OH	ErE	8	C2/c	5	c	0	2	1	
2 EuCl <sub>3</sub> ·2C <sub>4</sub> H <sub>10</sub> O <sub>4</sub> ·7H <sub>2</sub> O	EuE	9	P2/c	4	a	5		0	
		8		4	a	2		2	
NdCl <sub>3</sub> ·2.5C <sub>4</sub> H <sub>10</sub> O <sub>4</sub> ·C <sub>2</sub> H <sub>5</sub> OH	NdE(II)	9	P $\bar{1}$	8	a, d		0	1	
TbCl <sub>3</sub> ·1.5C <sub>4</sub> H <sub>10</sub> O <sub>4</sub> ·H <sub>2</sub> O	TbE(I)	8	P $\bar{1}$	5	a, d	1		2	
Ca(NO <sub>3</sub> ) <sub>2</sub> ·C <sub>4</sub> H <sub>10</sub> O <sub>4</sub>	CaEN	8	C2/c	4	a				2
Zn(NO <sub>3</sub> ) <sub>2</sub> ·C <sub>4</sub> H <sub>10</sub> O <sub>4</sub>	ZnEN	6	Cc	4	a				2
2La(NO <sub>3</sub> ) <sub>3</sub> ·C <sub>4</sub> H <sub>10</sub> O <sub>4</sub> ·8H <sub>2</sub> O	LaEN	11	P $\bar{1}$	2	a	3			3
Ln(NO <sub>3</sub> ) <sub>3</sub> ·C <sub>4</sub> H <sub>10</sub> O <sub>4</sub> ·2H <sub>2</sub> O	CeEN, PrEN	11	P2 <sub>1</sub> 2 <sub>1</sub> 2 <sub>1</sub>	3	b	2			3
Ln(NO <sub>3</sub> ) <sub>3</sub> ·C <sub>4</sub> H <sub>10</sub> O <sub>4</sub> ·C <sub>2</sub> H <sub>5</sub> OH	YEN, NdEN, EuEN, GdEN, TbEN	10	P2 <sub>1</sub> /c	3	b		1		3

<sup>a</sup>C. N., coordination number; Coordination modes of erythritol are as shown in Figure 8.

## CONCLUSION

New lanthanide ion-erythritol complexes were prepared and characterized using X-ray diffraction, FTIR, FIR, THz, and luminescence spectra. Two erythritol, one as two bidentate ligands, the other one as three hydroxyl group donor, coexist in the structure of the TbCl<sub>3</sub>-erythritol complex (TbE(I)). Four coordination structures were already observed for lanthanide chloride-erythritol complexes, but there is still one new structure (TbE(I)), which indicates the complexity of the coordination between hydroxyl groups and metal ions. Erythritol is a three-hydroxyl-groups donor in lanthanide nitrate-erythritol complexes, but two topological structures were observed depending on the existence of water or ethanol molecules and different lanthanide ions. Pr and Ce nitrate-erythritol complexes have water included in the coordination sphere; Y, Nd, Eu, Gd, and Tb ions can form complexes without water molecules. FTIR spectroscopy provides information about the coordination, the change of the ligand and hydrogen bonds; FIR spectra are related to M–O vibrations; THz bands are mainly lattice vibrations and hydrogen bonds; luminescence spectra are related to energy level transition. Combined with crystal structure results, these spectra demonstrate detailed information on the structure and coordination of these metal-carbohydrate complexes.

## ASSOCIATED CONTENT

### Supporting Information

Crystallographic data in CIF format for these lanthanide-erythritol complexes. This material is available free of charge via the Internet at <http://pubs.acs.org>.

## AUTHOR INFORMATION

### Corresponding Author

\*Telephone: 86-10-62751889. Fax: 86-10-62758849. E-mail: yanglm@pku.edu.cn; xyz@pku.edu.cn.

## ACKNOWLEDGMENTS

We gratefully acknowledge the financial support by National Natural Science Foundation of China for the grants (21001009 and 50973003), the State Key Project for Fundamental Research of MOST (2002CB713600 and 2011CB808304), and National High-tech R&D Program of China (863 Program) of MOST (2010AA03A406).

## REFERENCES

- (1) Davis, A. P.; Wareham, R. S. *Angew. Chem., Int. Ed.* **1999**, *38*, 2978–2996.
- (2) Whitfield, D. M.; Stojkovski, S.; Sarkar, B. *Coord. Chem. Rev.* **1993**, *122*, 171–225.
- (3) Angyal, S. J. *Adv. Carbohydr. Chem. Biochem.* **1989**, *47*, 1–43.
- (4) Burger, K.; Nagy, L. *Biocoordination Chemistry: Coordination Equilibria in Biologically Active Systems* **1990**, 236–283.
- (5) Umberto, P.; Carlo, F. *Prog. Inorg. Chem.* **1997**, *46*, 393–429.
- (6) Gyurcsik, B.; Nagy, L. *Coord. Chem. Rev.* **2000**, *203*, 81–148.
- (7) Yano, S.; Otsuka, M. *Metal Ions Biol. Systems* **1996**, *32*, 27–60.
- (8) Gottschaldt, M.; Schubert, U. S. *Chem.—Eur. J.* **2009**, *15*, 1548–1557.
- (9) Hartinger, C. G.; Nazarov, A. A.; Ashraf, S. M.; Dyson, P. J.; Keppler, B. K. *Curr. Med. Chem.* **2008**, *15*, 2574–2591.
- (10) Bowen, M. L.; Orvig, C. *Chem. Commun.* **2008**, *41*, 5077–5091.
- (11) Storr, T.; Obata, M.; Fisher, C. L.; Bayly, S. R.; Green, D. E.; Brudzinka, I.; Mikata, Y.; Patrick, B. O.; Adam, M. J.; Yano, S.; Orvig, C. *Chem.—Eur. J.* **2005**, *11*, 195–203.
- (12) Baran, E. J. *J. Inorg. Biochem.* **2009**, *103*, 547–553.

- (13) Vetter, C.; Pornsuriyasak, P.; Schmidt, J.; Rath, N. P.; Ruffer, T.; Demchenko, A. V.; Steinborn, D. *Dalton Trans.* **2010**, *39*, 6327–6338.
- (14) Li, G. H.; Badkar, A.; Kalluri, H.; Banga, A. K. *J. Pharm. Sci.* **2010**, *99*, 1931–1941.
- (15) Storr, T.; Merkel, M.; Song-Zhao, G. X.; Scott, L. E.; Green, D. E.; Bowen, M. L.; Thompson, K. H.; Patrick, B. O.; Schugar, H. J.; Orvig, C. *J. Am. Chem. Soc.* **2007**, *129*, 7453–7463.
- (16) Mikata, Y.; Shinohara, Y.; Yoneda, K.; Nakamura, Y.; Brudzinska, I.; Tanase, T.; Kitayama, T.; Takagi, R.; Okamoto, T.; Kinoshita, I.; Doe, M.; Orvig, C.; Yano, S. *Bioorg. Med. Chem. Lett.* **2001**, *11*, 3045–3047.
- (17) Taccardi, N.; Assenbaum, D.; Berger, M. E. M.; Bosmann, A.; Enzenberger, F.; Wolfel, R.; Neuendorf, S.; Goeke, V.; Schodel, N.; Maass, H.-J.; Kistenmacher, H.; Wasserscheid, P. *Green Chem.* **2010**, *12*, 1150–1156.
- (18) Garcia, I.; Marradi, M.; Penades, S. *Nanomedicine* **2010**, *5*, 777–792.
- (19) Su, Y. L.; Xu, Y. Z.; Yang, L. M.; Weng, S. F.; Soloway, R. D.; Wang, D. J.; Wu, J. G. *J. Mol. Struct.* **2009**, *920*, 8–13.
- (20) Song, Y. Y.; Xu, Y. Z.; Weng, S. F.; Wang, L. B.; Li, X. F.; Zhang, T. F.; Wu, J. G. *Biospectroscopy* **1999**, *5*, 371–377.
- (21) Kuzuya, A.; Machida, K.; Sasayama, T.; Shi, Y.; Mizoquchi, R.; Komiyama, M. *J. Alloy. Compd.* **2006**, *408*, 396–399.
- (22) Su, Y. L.; Xu, Y. Z.; Yang, L. M.; Yang, J.; Weng, S. F.; Yu, Z. W.; Wu, J. G. *Anal. Biochem.* **2005**, *347* (1), 89–93.
- (23) Albaaj, F.; Hutchison, A. J. *Int. J. Clin. Pract.* **2005**, *59*, 1091–1096.
- (24) Curran, M. P.; Robinson, D. M. *Drugs* **2009**, *69*, 2329–2349.
- (25) Angyal, S. J.; Craig, D. C. *Carbohydr. Res.* **1993**, *241*, 1–8.
- (26) Su, Y. L.; Yang, L. M.; Xu, Y. Z.; Wang, Z. M.; Weng, S. F.; Yan, C. H.; Wang, D. J.; Wu, J. G. *Inorg. Chem.* **2007**, *46*, 5508–5517.
- (27) Su, Y. L.; Yang, L. M.; Wang, Z. M.; Jin, X. L.; Weng, S. F.; Yan, C. H.; Yu, Z. W.; Wu, J. G. *Carbohydr. Res.* **2006**, *341*, 75–83.
- (28) Su, Y. L.; Yang, L. M.; Wang, Z. M.; Yan, C. H.; Weng, S. F.; Wu, J. G. *Carbohydr. Res.* **2003**, *338*, 2029–2034.
- (29) Su, Y. L.; Yang, L. M.; Wang, Z. M.; Weng, S. F.; Yan, C. H.; Wu, J. G. *J. Inorg. Biochem.* **2003**, *94*, 43–49.
- (30) Herdin, S.; Klufers, P.; Kunte, T.; Piotrowski, H. Z. *Anorg. Allg. Chem.* **2004**, *630*, 701–705.
- (31) Allscher, T.; Klufers, P. *Carbohydr. Res.* **2009**, *344* (4), 539–540.
- (32) Delangle, P.; Husson, C.; Lebrum, C.; Pecaut, J.; Vottero, P. J. A. *Inorg. Chem.* **2001**, *40*, 2953–2962.
- (33) Yang, L. M.; Zhao, Y.; Tian, W.; Jin, X. L.; Weng, S. F.; Wu, J. G. *Carbohydr. Res.* **2001**, *330*, 125–130.
- (34) Guo, J. Y.; Lu, Y. J. *Carbohydr. Chem.* **2010**, *29* (1), 10–19.
- (35) Lu, Y.; Deng, G. C.; Miao, F. M.; Li, Z. M. *Carbohydr. Res.* **2004**, *339* (10), 1689–1696.
- (36) Yang, L. M.; Wu, J. G.; Weng, S. F.; Jin, X. L. *J. Mol. Struct.* **2002**, *612*, 49–57.
- (37) Yang, L. M.; Zhao, Y.; Xu, Y. Z.; Jin, X. L.; Tian, W.; Weng, S. F.; Wu, J. G.; Xu, G. X. *Carbohydr. Res.* **2001**, *334*, 91–95.
- (38) Yang, L. M.; Tao, D. L.; Sun, Y.; Jin, X. L.; Zhao, Y.; Yang, Z. L.; Weng, S. F.; Wu, J. G.; Xu, G. X. *J. Mol. Struct.* **2001**, *560*, 105–113.
- (39) Yang, L. M.; Wang, Z. M.; Zhao, Y.; Tian, W.; Xu, Y. Z.; Weng, S. F.; Wu, J. G. *Carbohydr. Res.* **2000**, *329* (4), 847–853.
- (40) Yang, L. M.; Su, Y. L.; Xu, Y. Z.; Wang, Z. M.; Guo, Z. H.; Weng, S. F.; Yan, C. H.; Zhang, S. W.; Wu, J. G. *Inorg. Chem.* **2003**, *42*, 5844–5856.
- (41) Yang, L. M.; Xu, Y. Z.; Gao, X.; Zhang, S. W.; Wu, J. G. *Carbohydr. Res.* **2004**, *339*, 1679–1687.
- (42) Yang, L. M.; Xie, D. T.; Xu, Y. Z.; Wang, Y. L.; Zhang, S. W.; Weng, S. F.; Zhao, K.; Wu, J. G. *J. Inorg. Biochem.* **2005**, *99* (5), 1090–1097.
- (43) Yang, L. M.; Xu, Y. Z.; Wang, Y. L.; Zhang, S. W.; Weng, S. F.; Zhao, K.; Wu, J. G. *Carbohydr. Res.* **2005**, *340*, 2773–2781.
- (44) Yang, L. M.; Su, Y. L.; Xu, Y. Z.; Zhang, S. W.; Wu, J. G.; Zhao, K. *J. Inorg. Biochem.* **2004**, *98*, 1251–1260.

- (45) Yang, L. M.; Tian, W.; Xu, Y. Z.; Su, Y. L.; Gao, S.; Wang, Z. M.; Weng, S. F.; Yan, C. H.; Wu, J. G. *J. Inorg. Biochem.* **2004**, *98*, 1284–1292.
- (46) Sheldrick, G. M. SHELXS97, SHELXL97, Programs for Crystal Structures Solution and Refinement; University of Gottingen; Gottingen, Germany, 1997.
- (47) Hu, Y.; Wang, X. H.; Guo, L. T.; Zhang, C. L.; Liu, H. B.; Zhang, X. C. *Acta Phys. Sinica* **2005**, *54*, 4124–4128, (in Chinese).
- (48) Wu, J. G. *Modern Fourier Transform Spectroscopic Techniques and Its Applications*; Science and Technology References Press: Beijing, 1994.
- (49) Bekoe, A.; Powell, H. M. *Proc. R. Soc. London, Ser. A* **1959**, *250*, 301–315.
- (50) Nakamoto, K. *Infrared and Raman spectra of inorganic and coordination compounds*, 6th ed.; John Wiley & Sons: New York, 2009; pp 92–94.
- (51) Jesus, A. J. L.; Redinha, J. S. *J. Mol. Struct.* **2009**, *938*, 156–164.
- (52) Rozenberg, M.; Loewenschuss, A.; Lutz, H.-D.; Marcus, Y. *Carbohydr. Res.* **1999**, *315*, 89–97.
- (53) Rozenberg, M.; Loewenschuss, A.; Marcus, Y. *Carbohydr. Res.* **1997**, *394*, 183–186.
- (54) Yang, L. Q.; Wu, J. G.; Zhou, Q.; Bian, J.; Yang, Y. M.; Xu, D. F.; Xu, G. X. *Microchim. Acta* **1997**, *14*, 251–252.
- (55) Weng, S. F. *Fourier Transform Infrared Spectrometer*; Chemical Industry Press: Beijing, 2005, pp 270–272.
- (56) Yang, L. M.; Sun, H. Q.; Weng, S. F.; Zhao, K.; Zhang, L. L.; Zhao, G. Z.; Wang, Y. G.; Xu, Y. Z.; Lu, X. Y.; Zhang, C. L.; Wu, J. G.; Chen, J. E. *Spectrochim. Acta, Part A* **2008**, *69*, 160–166.
- (57) Yang, L. M.; Zhao, G. Z.; Li, W. H.; Liu, Y. F.; Shi, X. X.; Jia, X. F.; Zhao, K.; Lu, X. Y.; Xu, Y. Z.; Xie, D. T.; Wu, J. G.; Chen, J. E. *Spectrochim. Acta, Part A* **2009**, *73* (5), 884–891.
- (58) Xu, G. X. *Rare Earths*, 2nd ed.; Metallurgy Industry Press: Beijing, 1995; p 38.
- (59) Bian, J.; Liao, H.; Zhou, W. J.; Wu, J. G.; Xu, D. F.; Jiang, M.; Weng, S. F.; Shi, N.; Xu, G. X. Chinese Patent No CN1076958A, 1993-10-06.
- (60) Yu, L.; Hua, X. H.; Pan, Q. H.; Yang, L. M.; Xu, Y. Z.; Zhao, G. Z.; Wang, H.; Wang, H. Y.; Wu, J. G.; Liu, K. X.; Chen, J. E. *Carbohydr. Res.* **2011**, *346* (14), 2278–2284.